ELSEVIER

Thermochimica Acta 278 (1996) 165–173

thermochimica
acta

Dehydration kinetics of Wyoming montmorillonite studied by controlled transformation rate thermal analysis

Y. Laureiro[a], A. Jerez[b,*], F. Rouquérol[c], J. Rouquérol[d]

[a] *Departamento de Química Inorgánica-I, Facultad de Ciencias Químicas, Universidad Complutense, 28040-Madrid, Spain*
[b] *Departamento de Química Inorgánica y Química Técnica, Facultad de Ciencias, Universidad Nacional de Educación a Distancia, 28040-Madrid, Spain*
[c] *Laboratoire de Physicochemie des Interfaces, Case 2, Université de Provence, Place V. Hugo, 13331 Marseille Cedex 3, France*
[d] *Centre de Thermodynamique et Microcalorimétrie du CNRS, 26 rue du 141ème RIA, 13003 Marseille, France*

Received 20 December 1994; accepted 25 February 1995

Abstract

Controlled transformation rate thermal analysis (CRTA) is applied to the kinetic study of the thermal dehydration in vacuum of Wyoming montmorillonite. The release of water molecules takes place through successive diffusion processes and the Arrhenius parameters increase during the course of the dehydration reaction.

Keywords: Transformation rate thermal analysis; Montmorillonite; Arrhenius parameters; Dehydration reaction

1. Introduction

The smectite group consists of a number of clay minerals composed of tetrahedral–octahedral–tetrahedral silicate layers of both dioctahedral and trioctahedral types. Montmorillonite is by far the most abundant dioctahedral smectite. Its theoretical formula is $Al_2(SiO_{10})(OH)_2$ and the charge on the silicate layer is due to the replacement of Al^{3+} by Mg^{2+} in the octahedral sheet. Most montmorillonite specimens have additional substitution of Si^{4+} by Al^{3+} in the tetrahedral sheet as well as substitution of Al^{3+} by Fe^{3+} in the octahedral sheet. Exchangeable cations (charge balancing) exist between the silicate layers.

---

[*] Corresponding author.

SSDI 0040-6031(95)02330-5

The outstanding feature of the montmorillonite structure is that water (and other polar organic molecules) can enter between the unit layers causing the lattice to expand in the *c*-direction. The thickness of the water layers between the silicate units depends on the nature of the exchangeable cations at a given water vapour pressure [1]. This interlayer water, as well as the hydroxyl groups positioned in the clay structure, play an important role in the thermal behaviour of the smectite group in general [2].

Profiles of water release from this group on heating and dehydration kinetics based on isothermal or non-isothermal techniques have been reported [3–6].

Literature values for the activation energy of the dehydration and dehydroxylation processes of montmorillonites are quite variable. For instance, Tecilazic-Stevanovic et al. [7] reported a range of activation energies from 125 to 250 kJ mol^{-1}, depending on the hydration conditions and the exchangeable cation type.

Horvarth and Galikova [8] have studied the effect of exchangeable cations on dehydroxylation kinetics and found that montmorillonites with monovalent cations (except Na^+) dehydroxylated according to first-order kinetics, whereas the corresponding water release from montmorillonites with divalent cations was controlled by diffusional processes. (For the calcium form of the montmorillonite which they studied, an activation energy value of 110 kJ mol^{-1} was reported.)

More recently, a detailed study of the dehydroxylation kinetics of various montmorillonite specimens was carried out under isothermal conditions by Killingley and Day [9]. For the Wyoming montmorillonite, the subject of this work, they found that a D3 diffusion-controlled mechanism provided the best fit with the experimental data to about 80% reaction. The activation energy was determined as 333 kJ mol^{-1}.

In the present work, we studied the kinetics of thermal dehydration in vacuum of Wyoming montmorillonite by CRTA (controlled transformation rate thermal analysis). We have successfully applied this method, which was specially developed by J. Rouquérol [10] to lower at will the pressure and temperature gradients through the sample by an appropriate control of the reaction rate, to the kinetics of the thermal dehydrations of several compounds [11–14] under low water vapour pressure.

2. Experimental

2.1. Material

The Wyoming montmorillonite studied here was supplied by Ward's Natural Science Establishment Inc., Rochester, N. Y.

The structural formula of this mineral was reported to be $(Na_{0.64}K_{0.05}Ca_{0.03})(Si_{7.82}Al_{0.18})(Al_{3.06}Fe_{0.32}Mg_{0.65})O_{20}(OH)_4 \cdot nH_2O$ [15] and its cationic exchange capacity was determined as 92 meq per 10 g [16].

This sample was converted into the sodium form by treating the natural silicate repeatedly with a 1 N solution of NaCl and by dialysing until no Cl^- ions appeared in the dialysate. Only samples with particle size < 2 μm were used.

The *c*-spacing, measured by X-ray diffraction, is 1.13 nm. The nitrogen BET surface area was determined as 44 $m^2\ g^{-1}$ [17]. The total basal surface area deduced from crystallographic data, was 760 $m^2\ g^{-1}$.

2.2. Apparatus

The experiments were all carried out with fully automated and computerized controlled transformation rate evolved gas analysis (CR-EGA) equipment, which has been previously described [18] and operates between −30 and 1000°C. The residual pressure can be kept constant at any value ranging from 10^{-3} to 40 mbar.

2.3. Procedure

When using CRTA, an idea of the kinetic law involved is easily obtained by simply comparing the experimental curves (α vs. T) with a set of theoretical isokinetic curves constructed by Criado et al. [19], which can be split into 3 groups according to their general shape (see Fig. 1).

Kinetic analysis of the isokinetic data proceeds as follows [20]. The general equation of the reaction rate

$$d\alpha/dt = A\exp(-E/RT)f(\alpha) \tag{1}$$

simplifies, where $d\alpha/dt = C$ = constant, into

$$C/A = \exp(-E/RT)f(\alpha) \tag{2}$$

and hence

$$\ln(C/A) = -E/RT + \ln f(\alpha) \tag{3}$$

or

$$\ln f(\alpha) = E/RT + \ln(C/A) \tag{4}$$

Plots of $\ln f(\alpha)$ vs. $1/T$ are constructed for the functions describing the main mechanisms listed by Sharp et al. [21] (see Table 1) and the values of E and A are calculated from the linear regression coefficients. The best kinetic law would be that which gives the best correlation coefficient and the best agreement between the E value calculated as above and the value measured directly and independently by the rate-jump method [22] in the rate-jump method the reaction rate is cycled between two predetermined values (for instance in a ratio of 1 to 4), by increasing the gas flow

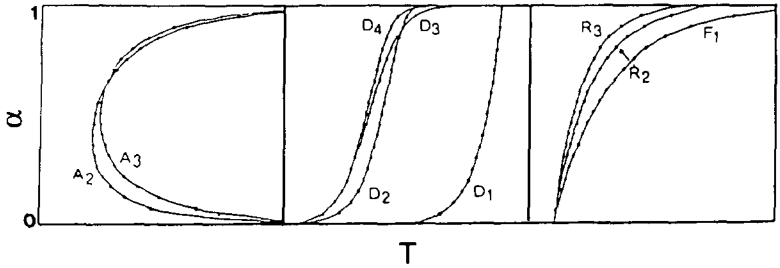

Fig. 1. Theoretical α versus T curves for CRTA.

Table 1
$f(\alpha)$ Functions for the most common mechanisms in heterogeneous kinetics (from Ref. [21])

Mechanism	Symbol	$f(\alpha)$
Unimolecular decay law	F1	$(1-\alpha)$
Two-dimensional phase boundary	R2	$2(1-\alpha)^{1/2}$
Three-dimensional phase boundary	R3	$3(1-\alpha)^{2/3}$
Two -dimensional random nucleation and growth of nuclei	A2	$2(1-\alpha)(-\ln(1-\alpha))^{1/2}$
Three-dimensional random nucleation and growth of nuclei	A3	$3(1-\alpha)(-\ln(1-\alpha))^{2/3}$
One-dimensional diffusion	D1	$1/2\alpha$
Two-dimensional diffusion	D2	$(-\ln(1-\alpha))^{-1}$
Three-dimensional diffusion (Jander equation)	D3	$3/2(1-\alpha)^{2/3}(1-(1-\alpha)^{-1/3})^{-1}$
Three-dimensional diffusion (Ginstling–Brounshtein equation)	D4	$3/2((1-\alpha)^{-1/3}-1)^{-1}$

towards the exterior of the reaction chamber in that ratio, and by measuring the resulting temperature limits. Each set of two successive rates with the corresponding temperatures allows an independent calculation of E from the equation

$$E=\frac{R\ln(4T_1T_2)}{T_2-T_1} \tag{5}$$

where T_1 and T_2 correspond to the same degree of reaction α.

3. Results and discussion

Fig. 2 reports the experimental CRTA curve obtained with a 23 mg montmorillonite sample decomposed under both a constant residual water vapour pressure of 6×10^{-3}mbar and a constant reaction rate $C=1.04\times10^{-5}\,\mathrm{s}^{-1}$.

As can be seen, this curve is more complicated than any of the theoretical curves given in Fig. 1 and although its S-shape can be correlated with that corresponding to the mechanisms controlled by diffusion, it is also possible to distinguish in this experimental curve some inflexions at certain temperatures (649, 697 and 743 K) which can be associated with changes in the mechanism and/or variations in the value of the Arrhenius parameters.

Between 743 and 913 K, the temperature increases very slowly and the curve does not show “discontinuity” in this temperature interval.

From 913 K, a sudden temperature increase and a sharp pressure drop indicate the end of the dehydration reaction under these experimental conditions.

These observations suggest that the release of water molecules takes place in different stages during dehydration of the sample. To verify these assumptions, we have performed the kinetic analysis over different temperature intervals by plotting the experimental data as $\ln f(\alpha)$ versus $1/T$. The result obtained are summarized in Tables 2–4.

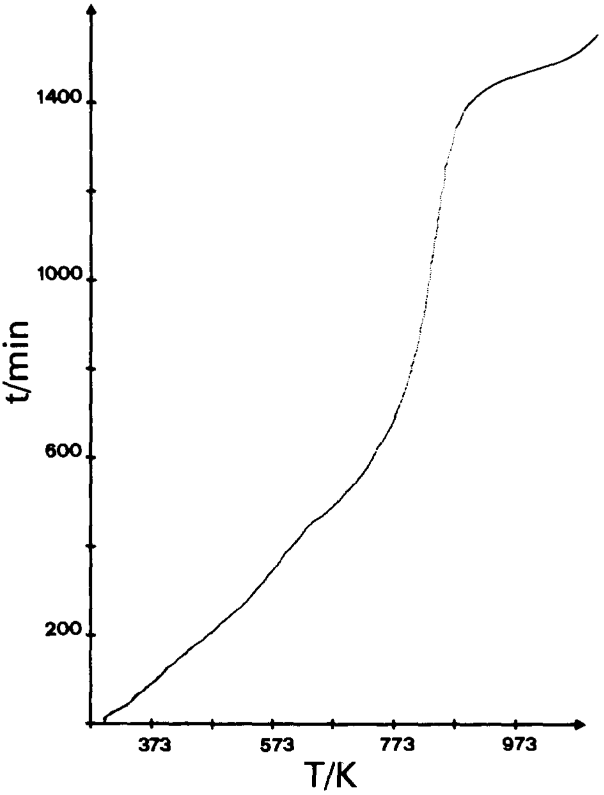

Fig. 2. Experimental CRTA curve obtained for Wyoming montmorillonite ($P_{H_2O} = 6 \times 10^{-3}$ mbar, $C = 1.04 \times 10^{-5} s^{-1}$).

Table 2
Kinetic analysis results obtained from the plot of Eq. (4) in the temperature interval 649 K $\leq T \leq$ 913 K

Mechanism	r	E/kJ mol^{-1}
F1	0.5763	64.3
R2	0.5763	32.2
R3	0.5763	42.9
A2	0.0026	8.7
A3	0.0033	9.8
D1	0.9406	86.9
D2	0.9708	111.2
D3	0.9310	144.3
D4	0.9614	122.9

As can be seen, the best correlation coefficients are obtained, in every case, for the diffusion laws, especially for the D2 and D4 mechanisms.

However, the fact that in the interval 743 K $\leq T \leq$ 913 K the correlation coefficients are closer to 1, seems to indicate that in this interval montmorillonite dehydration

Table 3
Kinetic analysis results obtained from the plot of Eq. (4) in the temperature interval 697 K $\leq T \leq$ 913 K

Mechanism	r	E/kJ mol^{-1}
F1	0.6537	94.6
R2	0.6537	74.3
R3	0.6537	63.1
A2	0.0081	21.3
A3	0.0002	13.1
D1	0.9016	111.4
D2	0.9655	146.7
D3	0.9532	195.5
D4	0.9685	163.9

Table 4
Kinetic analysis results obtained from the plot of Eq. (4) in the temperature interval 743 K $\leq T \leq$ 913 K

Mechanism	r	E/kJ mol^{-1}
F1	0.7692	152.4
R2	0.7692	76.2
R3	0.7692	101.6
A2	0.3361	63.4
A3	0.1206	33.7
D1	0.9183	122.5
D2	0.9919	178.1
D3	0.9813	256.8
D4	0.9959	215.6

obeys a single law, D2 or D4, which we cannot distinguish on the basis of the best mathematical fit. Nevertheless, given that the calculated E values are quite different for these mechanisms (178 and 215.6 kJ mol^{-1}, respectively) we can distinguish between them on the basis of the best agreement between these values and the value measured directly by applying the rate-jump method.

Fig. 3 reports the CRTA curve obtained on a 105 mg montmorillonite sample during a rate-jump experiment carried out under a constant residual pressure of 6×10^{-3} mbar (the same as that used in the previous experiment).

In this figure, the activation energies derived from each rate-jump, are also indicated which allows us to select the D4 mechanism as operative in the 743 K $\leq T \leq$ 913 K interval. The layer structure of the sample would be expected, in principle, to lead to a D2 mechanism. The fact that these kinetic laws are formulated from geometrical models, which have doubtful application to microcrystalline materials in which particles are orientated nearly at random, explains why a three-dimensional D4 mechanism provides the best fit with the experimental data.

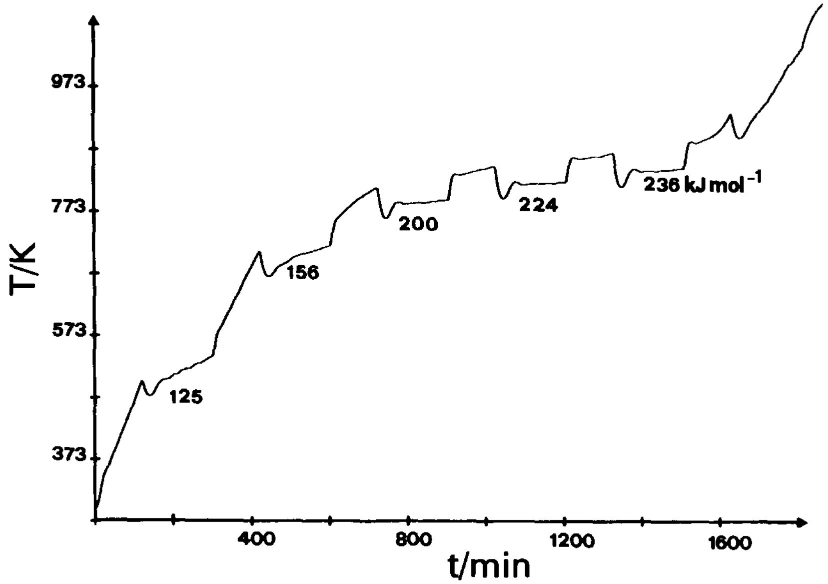

Fig. 3. Experimental CRTA curve obtained during a rate-jump experiment for Wyoming montmorillonite ($C_2 = 4C_1$, $P_{H_2O} = 6 \times 10^{-3}$ mbar).

However, the activation energy increases as the dehydration degree increases, although this energy increase is less marked in the 743 K $\leq T \leq$ 913 K interval over which, as we have already indicated, the mechanism does not change.

Fig. 4 reports the variation of the measured E values with the temperature during the dehydration process. Table 5 shows the variation of E with both the temperature and the degree of reaction α in the 743 K $\leq T \leq$ 913 K interval. In this table we have also included the pre-exponential factor values, which have been calculated for each α value using Eq. (4) in the particular case of a D4 law. A compensation effect is observed: be the pre-exponential factor also increases as the reaction proceeds.

This increase in the activation energy during the course of the dehydration process, which we have also observed [11] in other materials, can be associated with an increasing difficulty in the progress of the decomposition reaction.

Since this behaviour is not exceptional, but seems to be relatively frequent, the validity of "mean" parameters established by studies on the decomposition kinetics of materials such as the subject of this work, must be questioned.

4. Conclusions

The thermal dehydration of Wyoming montmorillonite carried out by CRTA under the experimental conditions indicated takes place through successive diffusion processes (as expected in view of the layer structure of the clay mineral). The kinetic analysis is most clearly defined in the 743 K $\leq T \leq$ 913 K interval.

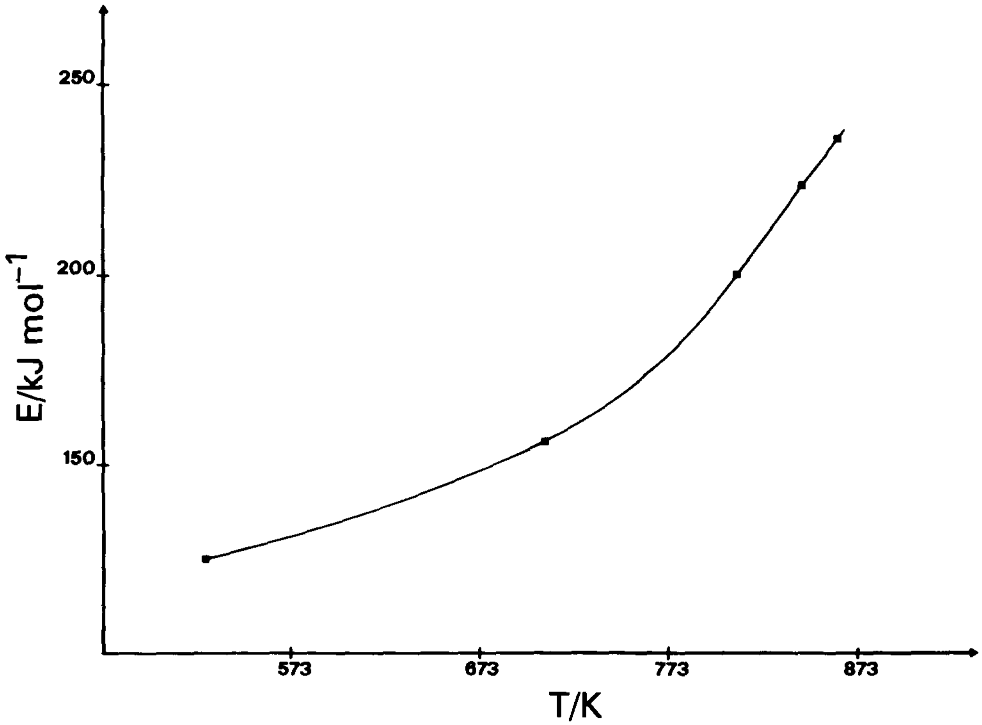

Fig. 4. Variation of measured E values with temperature during the dehydration process.

Table 5
Variation in the Arrhenius parameters, derived from the D4 law, with both temperature and degree of reaction in the 743 K $\leq T \leq$ 913 K interval

α	T/K	E/kJ mol^{-1}	A/s^{-1}
0.1	776	182	8.85×10^5
0.2	779	194	5.17×10^6
0.3	812	203	2.01×10^7
0.4	823	211	6.36×10^7
0.5	832	217	1.52×10^8
0.6	841	223	3.52×10^8
0.7	849	228	7.31×10^9
0.8	858	233	1.51×10^9
0.9	873	242	4.84×10^9

The activation energy increases in a uniform way as the degree of dehydration increases. This increase must be related to an increasing difficulty in the release of water molecules during the dehydration reaction. The pre-exponential factor also increases in parallel.

References

[1] R. Calvet, Bull. Soc. Chim. Fr., 8 (1972) 3097.
[2] C.M. Earnest, in W. Smykatz-Kloss and S.J. Warne (Eds.), Thermal Analysis in the Geosciences, 1990, Springer Verlag, Berlin, p. 134.
[3] J.D. Russel and V.C. Farmer, Clay Miner. Bull., 5 (1964) 443.
[4] C.M. Earnest, Perkin-Elmer Thermal Application Study #31, 1–8, Norwalk, CT, 1980.
[5] G. Andreotti, A. Loria, E. Mazzega and S. Valeri, Nuovo Cimento c, 1 (1978) 123.
[6] B.S. Girgis, N.S. Felix and K.A. El-Barawy, Thermochim. Acta, 112 (1987) 265.
[7] M.P. Tecilazic-Stevanovic, C.B. Nikolic and R.M. Munitlak, Glas. Hem. Drus. Beograd, 40 (1975) 521.
[8] I. Horvath and L. Galikova, Chem. Zvesti, 33 (1979) 604.
[9] J.S. Killingley and S.J. Day, Fuel, 69 (1990) 1145.
[10] J. Rouquérol, Thermochim. Acta, 144 (1989) 209.
[11] Y. Laureiro, A. Jerez, C. Pico and M.L. Veiga, Thermochim. Acta, 182 (1991) 47.
[12] Y. Laureiro, C. Pico, A. Jerez and M.L. Veiga, Thermochim. Acta, 184 (1991) 151.
[13] F. Rouquérol, Y. Laureiro and J. Rouquérol, Solid State Ionics, 63–65 (1993) 363.
[14] A. Ortega, F. Rouquérol, S. Akhouayri, Y. Laureiro and J. Rouquérol, Appl. Clay Sci., 8 (1993) 207.
[15] L.G. Shultz, Clays Clay Miner., 17 (1968) 115.
[16] E. Gutierrez, Ph. Thesis, Universidad Autónoma de Madrid, Madrid, 1989.
[17] J.E. Poirier, H. Francois, J.M. Cases and J. Rouquérol, in I.A. Liapis (Eds), Fundamentals of Adsorption, New York, 1987, p. 3.
[18] J. Rouquérol, S. Bordère and F. Rouquérol, Thermochim. Acta, 203 (1992) 193.
[19] J.M. Criado, A. Ortega and F. Gotor, Thermochim. Acta, 157 (1990) 171.
[20] S. Bordère, F. Rouquérol, J. Rouquérol, J. Estienne and A. Floreancing, J. Therm. Anal., 36 (1990) 1651.
[21] J.H. Sharp, G.W. Brindley and B.N.N. Achar, J. Am. Ceram. Soc., 49 (1966) 379.
[22] F. Rouquérol and J. Rouquérol, in H.G. Wiedemann (Ed.), Thermal Analysis, Vol. 1, Birkhäuser, Basel, p. 373.